DOR: 20.1001.1.27170314.2021.10.2.1.2

Research Paper

Numerical and Experimental Investigation of Thickness Distribution in Hydromechanical Deep Drawing Process of Square Parts

Farzad Rahmani[1], Seyed Jalal Hashemi[2*]
[1]Department of Mechanical Engineering, Kar Higher Education Institute, Qazvin, Iran
[2]Department of Mechanical Engineering, Faculty of Enghelab-e Eslami, Tehran Branch, Technical and Vocational University (TVU), Tehran, Iran
[*]Email of Corresponding Author: j_hashemi@tvu.ac.ir
Received: May 24, 2021; Accepted: July 30, 2021

Abstract
Hydromechanical deep drawing is a new process in sheet metal forming. In hydromechanical deep drawing, a chamber of fluid replaces the matrix and the final form of part is determined based on the form of rigid punch. This process can produce parts with more drawing ratios than traditional deep drawing. In this paper, the hydromechanical deep drawing (HDD) of square parts was studied using the finite element method (FEM), and the effects of different parameters of the process such as pre-bulging pressure, chamber pressure, and friction coefficient on the thinning were investigated. Simulation is done using Abaqus software. St12 sheets have been formed and the effect of parameters on thickness distribution is determined. A study was also carried out using an experimental setup to verify the FEM results. Results show that flange wrinkling decreases by increasing chamber pressure. Also selecting appropriate pre-bulging pressure can decrease the thinning significantly. Finally, the numerical results were compared with experimental data.

Keywords
Hydromechanical Deep Drawing, Drawing Ratio, Thinning

1. Introduction

The hydroforming of sheet metals, which has been developed widely in recent years, can replace a few of the metal forming methods. Advantages of this method, compared with traditional forming processes, are the ability to form of the complicated parts, increase of forming limit, the possibility of forming in one stage and then decreasing the number of production stages, higher quality of the produced parts, simplifying and increasing lifetime of the tools [1].

Recent studies on the optimization of process parameters have been focused on non-circular parts. Park et al. [2] studied the optimization process parameters for the parts with an oval cross-section. The effect of radius of punch and die in the deep drawing process has been studied by FEM and obtained results were compared with experimental results. Pegeta et al. [3] reported their work on achieving the optimum geometry of the blank for rectangular and circle parts in the deep drawing

process. They also considered the anisotropy and friction effects in the numerical study. Onder and Tekkaya [4] optimized the process parameters in the production of parts with different cross-sections by using hydromechanical deep drawing (HHD) and traditional deep drawing. PAMSTAMP was used to analyze the forming process. Zhang et al. [5] studied the wrinkling and rupture defects in the forming of parabolic parts by HDD process numerically and experimentally. According to achieved results, thinning takes place in the initial stages while wrinkling happens at the final stages of forming process. In another study [6], they analyzed the production of cone boxes with a rectangular section using the HDD method. The numerical analysis of the process was performed using LS-DYNA-3D then the local thinning, wrinkling configuration, and thickness distribution of the parts were studied. Aluminum and steel sheets were formed in the experimental study. Turkoz et al. [7] have been studied hydromechanical deep drawings of magnesium sheets at high temperatures. Ozturk et al. [8] have been used the fuzzy control approach in finite element simulation to find optimal loading conditions in hydromechanical deep drawing. Liu et al. [9] have been studied the effect of process parameters on wrinkling in hydromechanical deep drawing. Lang et al. [10] have been used heated media to increase the formability of aluminum sheets.

The most effective parameters on thinning in the HDD process for a specified drawing ratio are chamber pressure, pre-bulging pressure, pre-bulging height, and the distance between blank and blank-holder. The aim of this study is the analysis of the HDD process of square parts. The effect of pre-bulging pressure, friction coefficient, and blank thickness on thickness distribution would be investigated. Numerical results showed good adaption with experimental ones.

2. Process Modeling

Abaqus/CAE has been used to model the process tools and the forming process was simulated using Abaqus/Explicit. In the simulation, the effect of fluid pressure was modeled by applying pressure with uniform distribution. The changes of pressure are linear in the pre-bulging and forming stages (Figure 1). The material characteristics and process parameters used in the simulation are shown in Table 1. Die, punch, and blank-holder were modeled as a rigid surface. The friction coefficients between the blank and blank-holder (μ_h) were 0.05, between the blank and punch (μ_p) was 0.1, and between the blank and die (μ_d) was 0.05 which were considered as coulomb's friction law. The proper initial blank for deep drawing of the square section was applied on eight sides (Figure 2). The initial thickness of the blank was 1mm. The S4R element was used for meshing the blank. The whole blank contained 3621 nodes and 3500 elements. The drawing ratio was obtained by Equation 1.

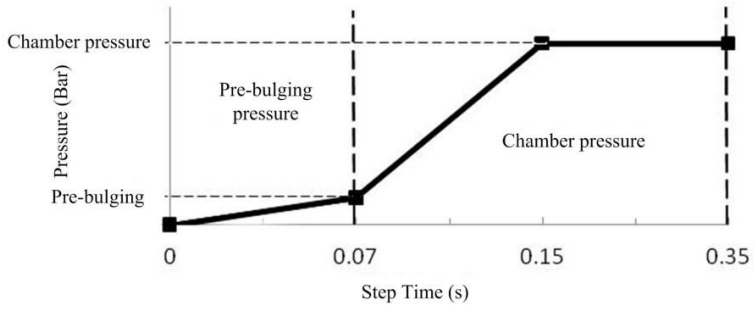

Figure 1: Chamber pressure in the forming step

Table 1: Material characteristics and process parameters

Property (unit)	value
Material	St12
Thickness (mm)	1
Yield stress (MPa)	294
Ultimate stress(MPa)	401
Density(g/cm^3)	7.8
Strength coefficient (MPa)	515
Work hardening exponent	0.22
Poisson ratio	0.3
Yang module (GPa)	210
Punch dimension (mm×mm)	150×150
Punch radius (mm)	37.5
Die dimension (mm×mm)	160×160
Size of spacer between the blank and blank-holder (mm)	1

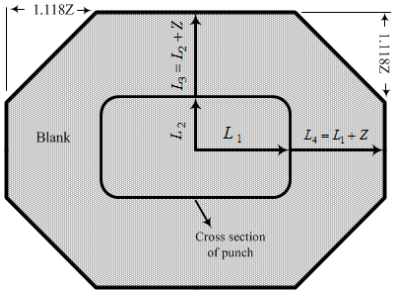

Figure 2: Initial blank shape

$$\beta_{eq}^2 = \frac{A_0}{A_m} \rightarrow A_0 = L_1 L_2 + 2L_1 Z + 2L_2 Z + 4Z^2 - 2.499848Z^2 \quad (1)$$

Where A_0 is the area of the initial blank and A_m is the average area of the punch section and die cavity. The height of the part (H) is calculated by Equation 2 considering that the volume of the sheet does not change in the forming process:

$$h = \frac{A_0 - A_m - A_f}{C_m} \quad (2)$$

Where A_f is the remaining area of the flange at the end of the process and C_m is the average perimeter of punch and die cavity.

3. Experimental Setup

An experimental setup of the HDD process was designed to verify the numerical results (Figure 3). The relief valve number 1 sets pre-bulging pressure while relief valve number 2 sets the chamber maximum pressure. At the pre-bulging stage, oil enters the chamber via pump 3, and chamber pressure would be increased. At the forming stage, the oil pressure would be increased severely by entering the punch into the die cavity. One-way valve prevents the reversion of oil and its discharge by the oil pump. After reaching the desired final limit of pressure, the operation continues at constant pressure.

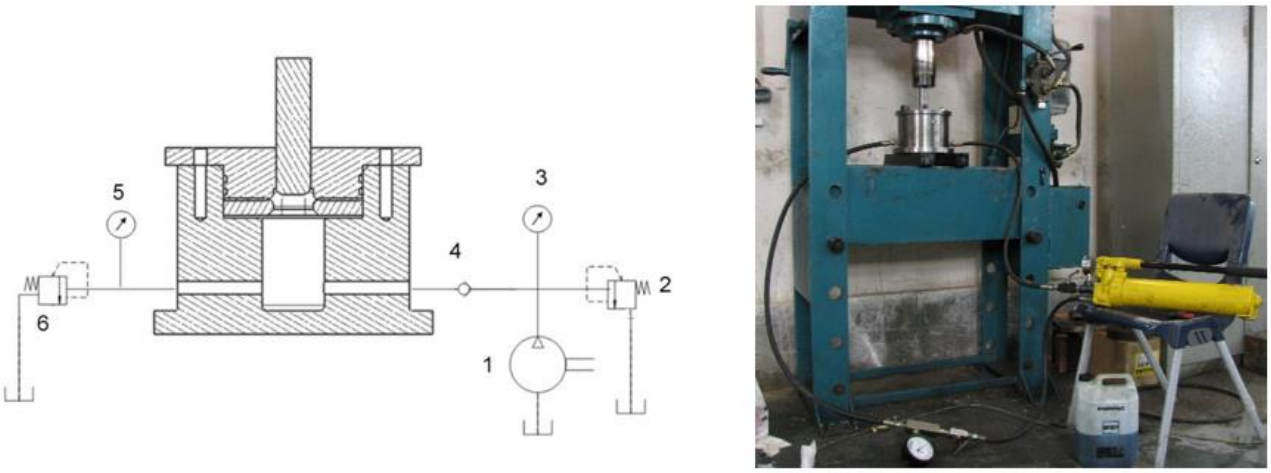

Figure 3. Experimental setup

The calculated diameters of blank and drawing height corresponding by different drawing ratios for square parts are shown in Table 2. Figure 4 displays the assembly of tools.

Table 2: Blank dimension and drawing depth for different drawing ratios

Drawing ratio	Drawing depth(mm)	Z(mm)
1.75	60.84	67.61
2	98.11	85.84
2.25	145.35	111.23

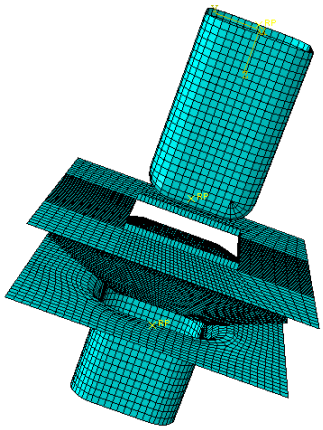

Fig. 4. Simulated tools

4. Results and Discussion

4.1 Effect of chamber pressure

Various simulations were carried out in final chamber pressure (P) of 50, 100, 150, 200, and 250 Bar to determine the effect of chamber pressure on the maximum of thinning. In all states, pre-bulging pressure (P_i) was considered 20 Bar. As shown in Figure 5, for two different drawing ratios (LDR),

the maximum of thinning increased at higher pressure. But increasing the chamber pressure decreased the wrinkling in the flange zone. Wrinkling in the flange zone is shown in Figure 6.

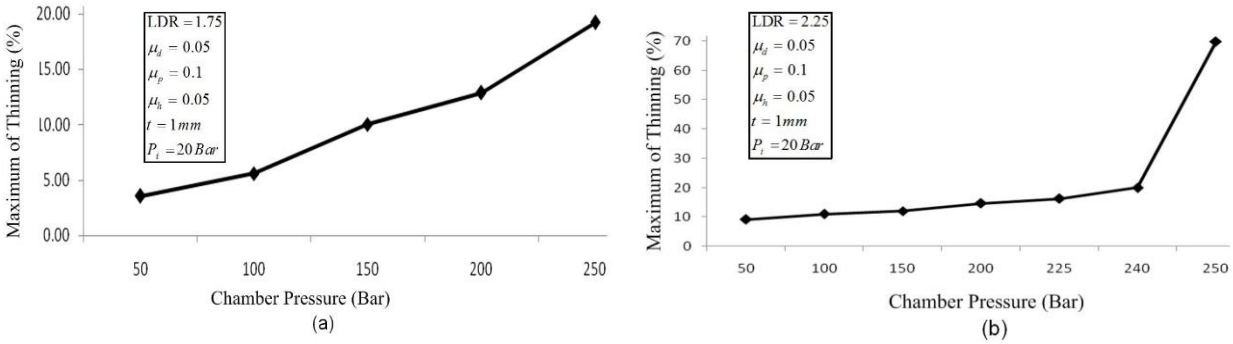

Figure 5 . Effect of chamber pressure on maximum of thinning (a) LDR= 1.75 (b) LDR= 2.25

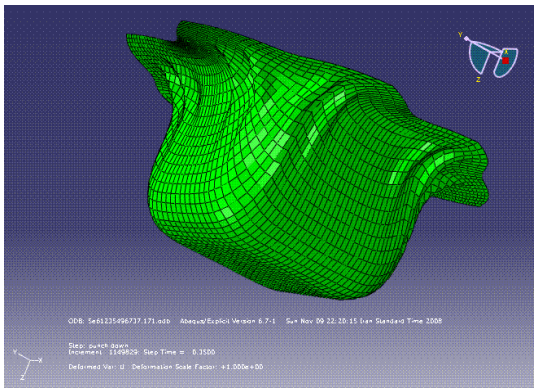

Figure 6. Wrinkling in the flange zone

Thickness distribution in the bottom, wall, and flange of part is shown in Figure 7. The bottom zone has lower thinning than other zones. A maximum of thinning is observed in the wall zone.

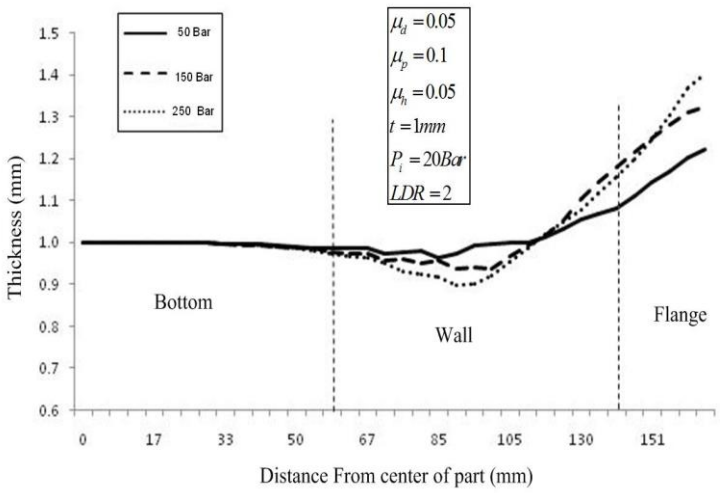

Figure 7. Thickness distribution of part in the bottom, wall, and flange

4.2. Effect of pre-bulging pressure

Keeping fixed the primary distance between punch and blank, various simulations were carried out to determine the effect of pre-bulging pressure on a maximum thinning. At lower pre-bulging

pressure, the blank doesn't bulge and cannot reach to punch, therefore the thinning increased. On the other hand, at higher pre-bulging pressure, the blank is subjected to more extension. As shown in Figure 8, a minimum of thinning is obtained using pre-bulging pressure between 20 to 35 Bar.

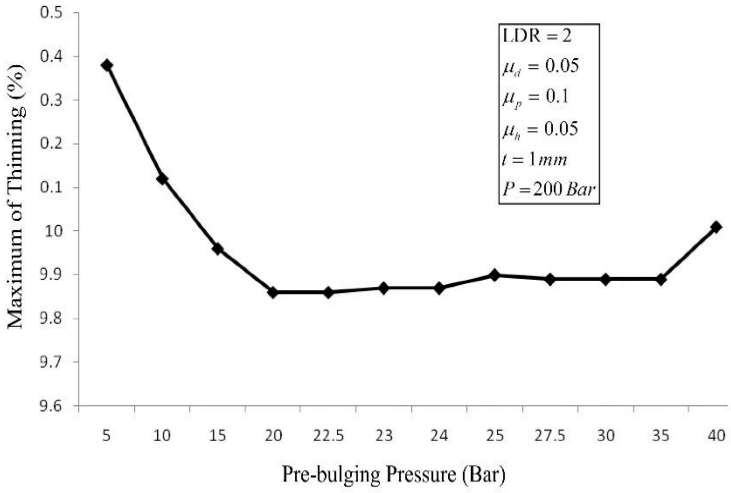

Figure 8. Thinning at various pre-bulging pressure

4.3 Effect of pre-bulging height

Pre-bulging height is the distance between the blank and punches before forming process. If the pre-bulging height increase, more extension will be induced in the sheet. The effect of the pre-bulging height on thinning is shown in Figure 9. There is an optimum value of pre-bulging height for each set of chamber pressure and pre-bulging pressure. At pre-bulging pressure of 35 Bar, pre-bulging height less than 5 mm is not appropriate. On the other hand, pre-bulging heights more than 5mm have higher thinning. Therefore, 5 mm is the optimum pre-bulging height approximately.

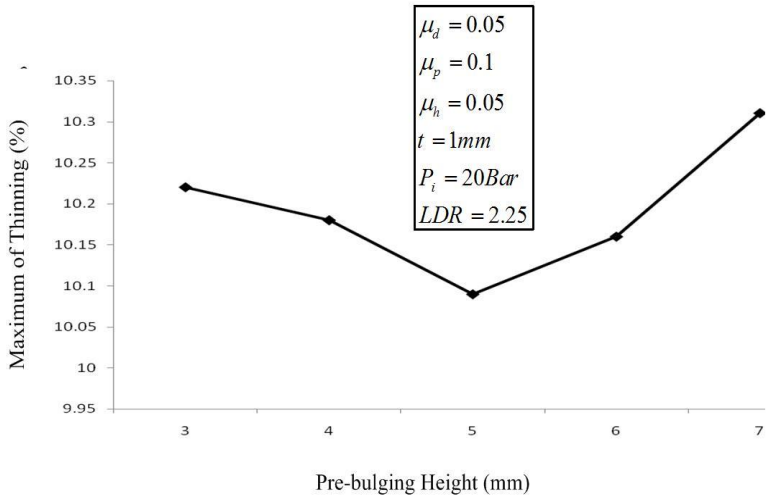

Figure 9. Effect of pre-bulging height on thinning

4.4 Comparison of numerical and experimental results

Thickness distribution obtained from numerical results is compared with experimental data in Figure 10(a). The thickness of the blank was 0.5 mm. as shown in Figure 10(a), there is good adaption between numerical and experimental results. The main reason for the small difference between numerical and experimental results is the error in friction coefficient applied in simulation. Octagon blanks prepared for various drawing ratios are shown in Figure 10(a). sound parts with different drawing ratios are shown in Figure 11.

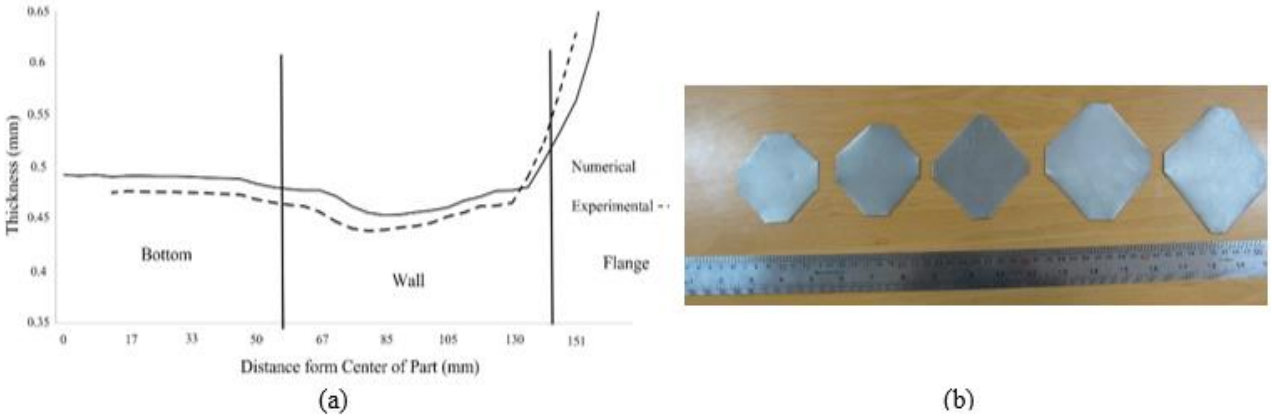

Figure 10. (a) comparison of numerical and experimental results (b) blanks for different drawing ratios

Figure 11. Perfect Parts in various drawing ratios

According to numerical results, in traditional deep drawing, failure occurs in the corner of the punch zone but in the HDD process, because of fluid pressure and friction force between sheet and punch wall, the probability of failure in the wall is more. Figure 12 shows a fracture in two traditional deep drawing and hydromechanical deep drawing processes.

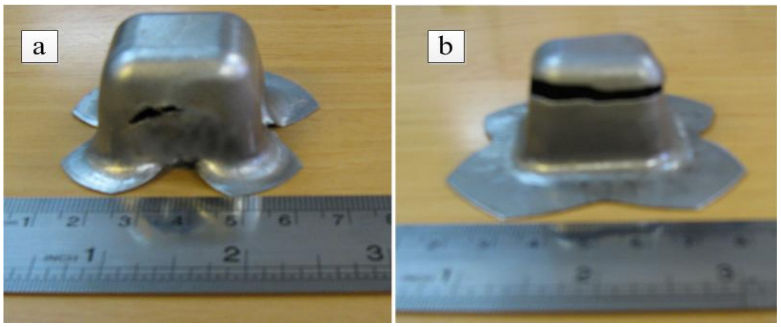

Figure 12. Failure in the parts; a) HDD and b) traditional deep drawing

5. Conclusion

In this paper, the forming limit of square parts in the deep drawing process was analyzed using both numerical and experimental approaches, and the effect of the process parameters such as chamber pressure, per-bulging pressure, pre-bulging height was investigated. Based on the results, low pre-bulging pressure led to more thinning in the wall of the part. There is an optimum pre-bulging height for each set of chamber pressure and pre-bulging pressure.

6. References

[1] Amino, H. and Nakagawa, T.1988. Application of Hydraulic Counterpressure Fluid Forming into Car Body Sheet Metal Forming. SAE Technical paper Series 880365, Int. Congr. and Expo., Detroit, MI: 35–48.

[2] Park, D.H., Kang, S.S. and Park, S.B. 2001. A study on the improvement of formability for elliptical deep drawing processes. Journal of Material Processing Technology. 113: 662-665.

[3] Pegada, V., Chun, Y. and Santhanam, S. 2002. An Algorithm for determining the optimum blank shape for the deep drawing of aluminum cups. Journal of Material Processing Technology. 125–126: 743–750.

[4] Onder, E. and Tekkaya, A.E. 2007. Numerical simulation of various cross sectional workpieces using conventional deep drawing and hydroforming technologies. International Journal of Machine Tools & Manufufacturing. 48: 532-542.

[5] Zhang, S.H. and Danckert, J. 1998. Development of hydro-mechanical deep drawing. Journal of Material Processing Technology. 83: 14-25.

[6] Zhang, S.H., Lang, L.H., Kang, D.C., Danckert, J. and Nielsen, K.B. 2000. Hydromechanical deep-drawing of aluminum parabolic workpieces-experiments and numerical simulation. International Journal of Machine Tools & Manufacturing. 40: 1479-1492.

[7] Türköz, M., Cora, Ö.N., Gedikli, H., Dilmeç, M., Halkacı, H.S. and Koç, M. 2020. Numerical optimization of warm hydromechanical deep drawing process parameters and its experimental verification. Journal of Manufacturing Processes. 57: 344-353.

[8] Öztürk, E., Türköz, M., Halkacı, H.S. and Koç, M., 2017. Determination of optimal loading profiles in hydromechanical deep drawing process using integrated adaptive finite element analysis and fuzzy control approach. The International Journal of Advanced Manufacturing Technology. 88(9-12): 2443-2459.

[9] Liu, W., Xu, Y. and Yuan, S. 2014. Effect of pre-bulging on wrinkling of curved surface part by hydromechanical deep drawing. Procedia Engineering. 81: 914-920.

[10] Lang, L., Liu, B., Li, T., Zhao, X. and Zeng, Y. 2012. Experimental investigation on hydromechanical deep drawing of aluminum alloy with heated media. steel research international. 83(3): 230-237.